



A Technique for Determining Thermal Transport Properties of Small, Electrically Conductive Liquid or Solid Specimens

by Michael McQuaid and Max Cohen

ARL-TR-1905

March 1999

Approved for public release; distribution is unlimited.

19990827 035

The findings in this report are not to be construed as an official Department of the Army position unless so designated by other authorized documents.

Citation of manufacturer's or trade names does not constitute an official endorsement or approval of the use thereof.

Destroy this report when it is no longer needed. Do not return it to the originator.

Army Research Laboratory

Aberdeen Proving Ground, MD 21005-5066

ARL-TR-1905**March 1999**

A Technique for Determining Thermal Transport Properties of Small, Electrically Conductive Liquid or Solid Specimens

Michael McQuaid and Max Cohen

Weapons and Materials Research Directorate, ARL

Abstract

The experimental approach developed by Miller and Kotlar for determining the thermal conductivity and thermal diffusivity of small, solid, energetic-material specimens—"Technique for Measuring the Thermal Diffusivity/Conductivity of Small Thermal Insulator Specimens," *Review of Scientific Instruments*, vol. 64, pp. 2954–2960, 1993—has been modified and extended for use in determining these properties for electrically conductive materials, including liquids. As in the technique developed by Miller and Kotlar, these properties are determined from the transient temperature response of a point in an experimental system consisting of two "semi-infinite" media, a plane of which is subjected to a well-defined heat flux. However, to allow the technique to be employed with electrically conductive specimens, the experiment is configured so that the heat flux is generated at a plane in a nonconductive solid (as opposed to the interface between the media), and the temperature response is measured in this solid as well. The parameter $(\lambda\rho c_p)^{1/2}$ is obtained by fitting a numerical simulation of the heat transfer process to the temperature response. Coupling the model to a nonlinear least-squares fitting routine facilitates this effort. To obtain absolute values for the specimen's thermal conductivity and thermal diffusivity, knowledge of its density and heat capacity is required. The viability of the experimental approach was established through experiments with water, methanol, and ethylene glycol, and the technique was employed to obtain the thermal conductivity of liquid propellant XM46 for temperatures in the range 20–60° C.

Acknowledgments

The authors would like to thank Dr. M. Miller for the use of his experimental apparatus, his guidance in its operation, and helpful discussions regarding the interpretation of results. We are also indebted to Dr. A. Kotlar for his help in understanding the interdependence of parameters employed in fitting the experimental data, to Dr. A. Birk for reviewing this report, and to Dr. R. Beyer for arranging Mr. Cohen's internship and supporting this effort.

INTENTIONALLY LEFT BLANK.

Table of Contents

	<u>Page</u>
Acknowledgments.....	iii
List of Figures	vii
List of Tables	ix
1. Introduction	1
2. Experimental Considerations.....	5
3. The Heat Transfer Process and Data Reduction Considerations	8
4. Results	12
5. Discussion.....	15
6. Summary	20
7. References	21
Appendix: Numerical Simulation of the Heat Transfer Process	23
List of Abbreviations.....	29
Distribution	31
Report Documentation Page.....	33

INTENTIONALLY LEFT BLANK.

List of Figures

<u>Figure</u>	<u>Page</u>
1. Schematic Diagram of Experimental Setup Employed by Miller and Kotlar [1]	2
2. Schematic Diagram of Experimental Setup Employed by McQuaid et al. [4] for Studying Pyrotechnics	2
3. Schematic Diagram of Experimental Setup Employed for the Current Study.....	2
4. Voltage vs. Time Plot Associated With the Heat Generation Pulse	11
5. Temperature Response Observed in an Experiment With Water and the Fit of the Numerical Model to These Data.....	13
6. Plot of Measured Thermal Conductivity Values vs. Recommended Literature Values for Water, Ethylene Glycol, and Methanol	13
7. Measured Thermal Conductivity Values for XM46 and Water in the Range 20–60° C.....	16
8. Spatial Temperature Profiles as a Function of Time for a Model System With a Fused Silica Sample ($f_o = 0.25 \text{ W/cm}^2$)	17
9. Spatial Temperature Profiles as a Function of Time for a Model System With a Methanol Sample ($f_o = 0.25 \text{ W/cm}^2$)	17
10. Temperature vs. Time Responses at the Thermocouple for Various Model Systems: (a) "Fused Silica," $\lambda = 12.0 \text{ mW/cm-}^\circ\text{C}$, $r_f = 0.33 \text{ } \Omega$; (b) "Water," $\lambda = 6.1 \text{ mW/cm-}^\circ\text{C}$, $r_f = 0.33 \text{ } \Omega$; (c) "Water," $\lambda = 6.1 \text{ mW/cm-}^\circ\text{C}$, $r_f = 0.34 \text{ } \Omega$; and (d) Fit to Simulation (c) Assuming $r_f = 0.33 \text{ } \Omega$, the Fitting Routine Finding $\lambda = 4.8 \text{ mW/cm-}^\circ\text{C}$	18
A-1. Pictorial Representation of Numerical Model Parameters.....	26

INTENTIONALLY LEFT BLANK.

List of Tables

<u>Table</u>	<u>Page</u>
1. Physical Properties of Selected Fluids at or Near 25° C	8

INTENTIONALLY LEFT BLANK.

1. Introduction

The thermal transport properties of an unreacted energetic material determine how thermal energy from various heat sources distributes in the material as it functions. Given the coupling between thermal energy and the kinetics of chemical energy release, these properties will play an important role in the way a material performs. For example, the thermal transport properties of a propellant will dictate how quickly a surface subject to an initiation stimulus will reach ignition threshold temperatures, and how the subsequent heat of combustion feeds back into the material. As such, thermal transport underlies ballistic-controlling phenomena such as ignition delay and burning rate behavior. In liquids, thermal transport properties also influence how shear-induced heating is dissipated. Shear-induced heating has been implicated as a mechanism of inadvertent ignition in developmental liquid propellant gun propulsion systems, and transport properties are required for computational fluid dynamic (CFD) simulations employed to address vulnerability issues in such systems. However, few thermal transport property measurements have been published for energetic materials in general, and liquids in particular. This deficiency stems in part from the experimental difficulty attending the measurement of thermal transport properties using small specimens. Small specimen sizes are often dictated by the grain geometry of (solid) materials and are extremely desirable from the standpoint of safety.

To facilitate the measurement of the thermal transport properties of small specimens, Miller and Kotlar (MK) [1, 2] developed an experimental technique (shown schematically in Figure 1) in which a well-defined heat flux is generated at the interface between an (energetic) specimen and a second material with known thermal transport properties. (Figures 2 and 3 show modifications of their technique that are described later.) They showed that the experimental system approaches the mathematical idealization of a step-function heat flux generated at the interface of two "semi-infinite" media. In this idealization, the temperature response, in the energetic specimen at a known distance from the interface (x) is given as a function of time (t) by [3]

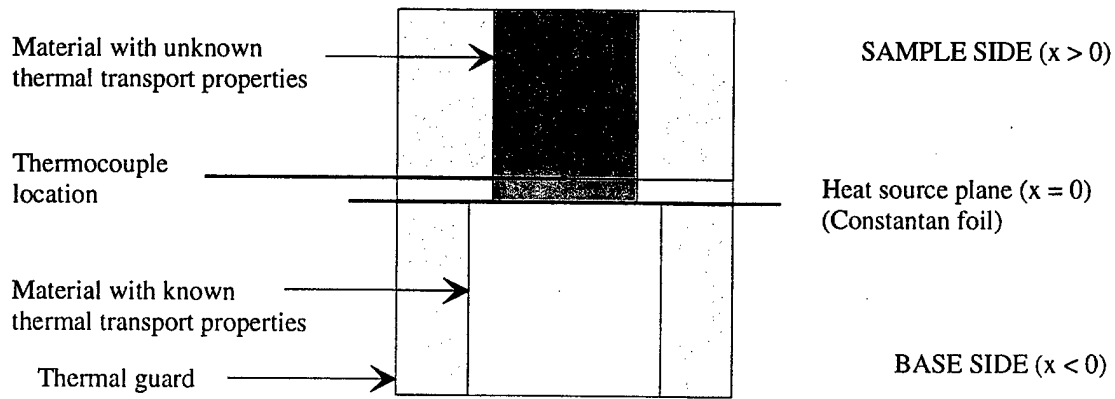


Figure 1. Schematic Diagram of Experimental Setup Employed by Miller and Kotlar [1].

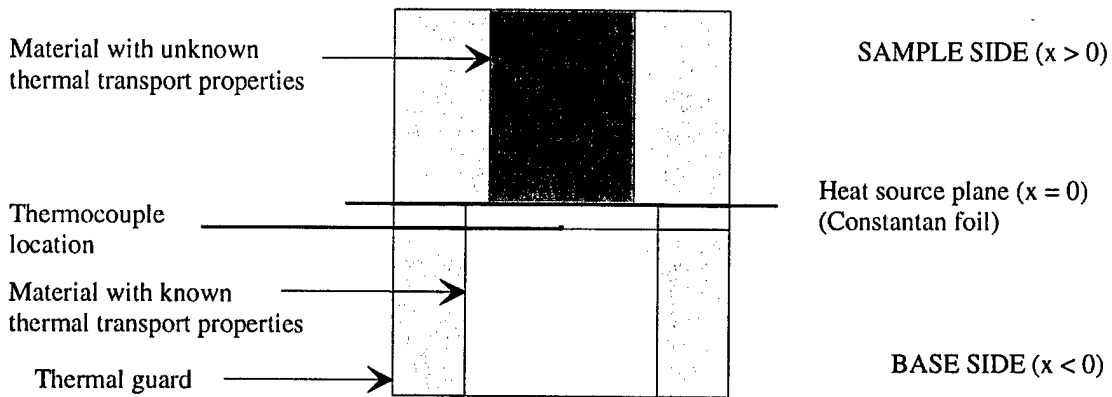


Figure 2. Schematic Diagram of Experimental Setup Employed by McQuaid et al. [4] for Studying Pyrotechnics.

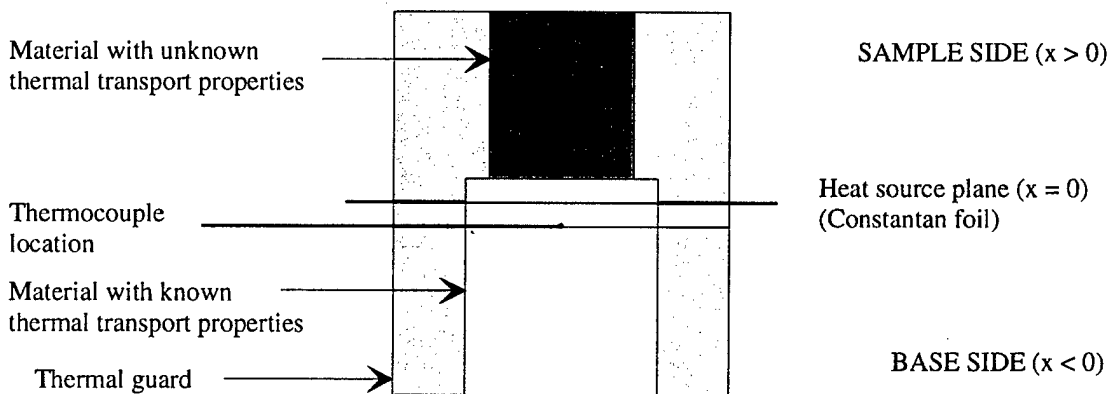


Figure 3. Schematic Diagram of Experimental Setup Employed for the Current Study.

$$T(x,t) = T_o + \frac{2f_o\sqrt{\alpha_s\alpha_bt}}{\lambda_b\sqrt{\alpha_s} + \lambda_s\sqrt{\alpha_b}} \text{ierfc}\left(\frac{x}{2\sqrt{\alpha_st}}\right), \quad (1)$$

where f_o is the heat flux, T_o is the ambient temperature, and α_s (α_b) and λ_s (λ_b) are the thermal diffusivity and thermal conductivity of the sample (base), respectively. The function $\text{ierfc}(x/2(\alpha_st)^{1/2})$ is the complementary error function integral. Fitting this function to the experimental data yields, simultaneously, the thermal conductivity and thermal diffusivity of the specimen. With this technique, Miller was able to establish thermal conductivity and thermal diffusivity values for a number of solid gun propellant formulations and RDX [5–8].

While the MK technique offers a valuable tool for measuring the thermal transport properties of small, solid samples, there are certain aspects of the approach that limit its range of applicability. Because the technique is based on measuring the temperature response at a point in the sample, a technique for preparing a thin wafer of the material is required. One technique is to wafer a stock piece using a low-speed saw. However, this is untenable for crumbly formulations and will alter a compound's properties if the cutting fluid preferentially leaches one of its constituents. An alternative technique is to press a sample into a specimen of the desired thickness. However, there is some question as to whether a specimen produced in this manner will be representative of an actual grain of the material. Also, the use of the technique with electrically conductive materials is problematic. Because the temperature response is measured with a thermocouple and the heat flux is generated by resistively heating a metallic foil, electrically conductive materials will allow leakage of current through the material to the thermocouple. Such current will influence the thermocouple readout, and the path through the specimen has the potential to act as an ignition source.

To address these issues when they arose during a study to characterize the thermal transport properties of pyrotechnic materials, McQuaid et al. [4] employed a slight modification of the MK technique—namely, measuring the temperature response in the base instead of the sample (see Figure 2). This approach precludes the need to prepare thin samples and allows the apparatus to

be used for materials that are slightly electrically conductive. (Highly electrically conductive materials are still problematic because the alternate electrical path afforded by the material compromises one's ability to characterize the heat flux.) Moreover, this configuration facilitates the testing of a series of samples because, once in place, the delicate thermocouple does not have to be handled again. However, the benefits accrued through this approach come with a significant price—namely, that the function describing the temperature response becomes

$$T(x,t) = T_o + \frac{2f_o\sqrt{\alpha_s\alpha_b t}}{\lambda_b\sqrt{\alpha_s} + \lambda_s\sqrt{\alpha_b}} \operatorname{ierfc}\left(\frac{x}{2\sqrt{\alpha_b t}}\right) \quad (2a)$$

or

$$T(x,t) = T_o + \frac{2f_o\sqrt{t}}{\lambda_b/\sqrt{\alpha_b} + \lambda_s/\sqrt{\alpha_s}} \operatorname{erfc}\left(\frac{x}{2\sqrt{\alpha_b t}}\right), \quad (2b)$$

and in fitting this function to the experimental data, the thermal diffusivity (α_s) and thermal conductivity (λ_s) of the sample are no longer mathematically independent parameters. Instead, the parameter derivable from the experiment is the ratio $\lambda_s/(\alpha_s)^{1/2}$, which, applying the definition $\alpha_s = \lambda_s/\rho c_p$, is equal to $(\lambda_s\rho c_p)^{1/2}$, where ρ and c_p are the specimen's density and heat capacity, respectively. Thus, it is necessary to know the specimen's ρ and c_p to get absolute values for λ_s and α_s . While the density is a relatively easy property to measure, heat capacity measurements are a nontrivial extra step.

Having demonstrated that measurement of the temperature response in the base could be used as a basis for deriving thermal conductivity values of a solid specimen, the possibility of obtaining such values for liquids was suggested. The impetus to proceed was a curiosity about the thermal conductivity of liquid propellant XM46 (60.79 weight-percent hydroxylammonium nitrate, 19.19 weight-percent triethanolammonium nitrate, and 20.02 weight-percent water). Though a wide variety of its physical properties have been characterized, only one study of its thermal conductivity could be found [9], and the reported uncertainty in the values was relatively large. We were also aware of the need for establishing the thermal transport properties of fluids being

considered for use in the recoil system of a developmental lightweight howitzer and anticipate the need to establish such values for new propellant formulations. Thus, the development of an in-house capability for making such measurements was considered desirable. This report describes the development of the technique and its application in establishing the thermal conductivity values of XM46 for temperatures in the range 20–60° C.

2. Experimental Considerations

MK have discussed the difficulty of measuring the thermal conductivity and thermal diffusivity of small solid samples, and their technique elegantly addresses typical concerns such as the generation of a well-defined (step function) heat flux, the spatial uniformity of flux, the match between experimental and model boundary conditions, and instrumentation errors [1, 2, and 10]. For liquids, the technique generally considered most accurate for obtaining the thermal conductivity of electrically nonconducting materials is the transient hot-wire technique [11]. This technique involves heating a bare metallic wire/resistance thermometer in a bath of the liquid of interest, and the temperature response of the wire is analyzed to obtain the thermal conductivity. However, if the wire is in contact with an electrically conductive fluid, current will flow through both the fluid and the wire, compromising the experimenter's ability to characterize the heat flux. One approach to addressing this issue is to coat the wire with a nonconductive material. Though simple in principle, these experiments are highly demanding, and we were interested in developing a single technique for both liquids and solids using available equipment. Modifying the MK technique offered such a possibility.

Perhaps the biggest obstacle to applying the MK technique to the measurement of liquids has to do with the fact that the distance between the (foil) heat source and the thermocouple has to be known precisely (e.g., 0.0400 ± 0.0005 cm), and such precision is unlikely to be obtained unless the thermocouple is supported by a rigid structure. Locating the thermocouple in the base as done by McQuaid et al. [4] meets this requirement. Allowing direct contact between the foil and sample also presents difficulties. For the experiment to approach the idealization described—i.e.,

that the heat flux emanate from a plane of zero [thermal] mass—the constantan foil that is resistively heated to produce the heat flux must be thin (0.0005 cm thick), and it is easily torn. It would be difficult to fabricate it into a leak-proof container bottom or to clean it upon changing specimens. Based on this concern, it was decided to employ a sample container with a bottom fabricated from the same material as the base. Not only does this provide a rugged component, with the proper choice of material, it can act as an electrical insulator, allowing the technique to be used with highly electrically conductive materials.

The basic hardware used in this study was the same as that employed by Miller and described in detail in MK [1, 2]. Briefly, a 4.4-cm-long, 1.2-cm-wide, 0.0005-cm-thick constantan foil (Hamilton Precision Metals) is resistively heated via a voltage-regulated power supply (Hewlett-Packard, Model 6024A), generating a step increase in current when the circuit is closed via a mercury-wetted relay. The consequent heat flux sends thermal waves into the adjacent test pieces, and the temperature response at a known distance from the foil is monitored with a bare Chromel/Alumel thermocouple (Omega, Style II). The output of the thermocouple is preamplified via a differential amplifier (Stanford Research Systems, Model SR560) and recorded with a digital oscilloscope (Nicolet, Model 4094/4570) over a 4-s period. This period includes a 0.4-s period prior to flux onset, providing an unbiased window on the ambient temperature. A data point is acquired every 0.002 s over the data acquisition period. Toward determining the heat flux generated by the foil, $f_o(0,t)$, the voltage difference, $V(t)$, between the electrodes holding the foil is recorded on a channel of the digital oscilloscope, and a nominal value for the current in the foil, I_o , is obtained from the readout of a multimeter (Fluke, Model 77). The temperature of the test fixture was controlled by circulating a 50/50 ethylene glycol-water mixture from a temperature-controlled bath (Neslab, Model ULT-80DD) through copper tubing soldered to the copper block housing the fixture.

Figure 3 is a schematic diagram of the experimental configuration employed in this study. For the results reported here, the container bottom, the wafer inserted between the foil and the thermocouple, and the base were cut from a 1.3-cm-long, 1.3-cm-diameter fused silica cylinder of unknown origin. (MK had employed acrylic for the base material, and preliminary

experiments with tests pieces constructed from this material were conducted in this study. But some of the fluids being tested were found to permeate the acrylic.) To construct the base, the fused silica cylinder was epoxied into a 1.9-cm outside diameter (OD), 1.3-cm inside diameter (ID) acrylic tube, and two wafers approximately 0.043 cm thick were cut from the assembly. (This was about the thinnest wafer that could be fabricated without the assembly falling apart or the fused silica breaking.) The thermocouple and a very thin layer of thermal conductivity paste was placed between one wafer and the base, and the assembly was held together by solvent welding the acrylic pieces together. To construct the sample container, the other wafer was epoxied to a 1.9-cm-OD, 0.9-cm-ID, 1-cm-long acrylic tube.

The thermal diffusivity and thermal conductivity of the fused silica employed for the base material, which are needed as input to the model of the heat transfer process, were established by conducting experiments in which the sample side was occupied by a fused silica specimen from the same lot as that used to construct the base. This configuration permits a direct measure of the parameters without *a priori* knowledge of their value. Values were obtained for a temperature range 20–60° C, and the linear least-squares fit of these data found $\lambda = 12.055 - 0.000084T$ mW/cm-°C and $\alpha = (7.6957 - 0.0214T) \times 10^{-3}$ cm²/s, where T is in degrees Celsius. These equations yield values for fused silica that are similar to those reported by MK [1, 2].

In order to establish the viability of the experimental approach, tests were conducted with water, ethylene glycol, and methanol. These liquids were chosen because they are relatively innocuous and their thermal transport properties are available in the literature (see Table 1). For the tests reported here, the water sample was drawn from a commercial still. The methanol (Fisher Scientific, ≥99.9% stated purity), ethylene glycol (Fisher Scientific, Laboratory Grade, unknown purity), and XM46 (Thiokol, Lot 5) were used as supplied. For the experiments with these liquids, the container was filled nearly to the top (i.e., approximately 0.9 cm deep) with the sample of interest and covered with a thin acrylic lid. The lid allowed a tensioning spring

Table 1. Physical Properties of Selected Fluids at or Near 25° C

Fluid	Thermal Conductivity ^a (mW/cm-°C)	Density ^b (g/cm ³)	Heat Capacity ^b (J/g-°C)
Water	6.08	1.00	4.18
Ethylene Glycol	2.57	1.11	2.43
Methanol	2.02	0.79	2.55
XM46	—	1.43 ^c	2.53 ^d

^a Values recommended in IFI [12].

^b Except as noted, values recommended in Perry and Chilton [13].

^c Messina et al. [9].

^d Messina [14].

and a screw to apply pressure to the container, ensuring good contact between the container bottom and the foil.

3. The Heat Transfer Process and Data Reduction Considerations

In developing their experiment, MK addressed issues related to whether the experiment can be analyzed with a 1-D model, the primary concern being the radial extent of system components. Since our samples had a greater diameter than those employed in their study, a 1-D model is considered warranted here. For a system with a base of thickness l_b occupying $-l_b \leq x \leq 0$, a container bottom of thickness l_c occupying $0 \leq x \leq l_c$, and a specimen of thickness l_s occupying the range $l_c < x < l_c + l_s$, the governing equations for the heat transfer process associated with a total heat flux, $f_o(0,t)$, are

$$\frac{\partial T(x,t)}{\partial t} = \alpha_b \frac{\partial^2 T(x,t)}{\partial x^2}, \quad -l_b < x < l_c \quad (3a)$$

and

$$\frac{\partial T(x,t)}{\partial t} = \alpha_s \frac{\partial^2 T(x,t)}{\partial x^2}, \quad l_c < x < l_c + l_s, \quad (3b)$$

with boundary conditions

$$T(x,0) = T_o; \quad -\infty < x < +\infty, \quad (3c)$$

$$\lambda_b \frac{\partial T(l_c^-, t)}{\partial x} = \lambda_s \frac{\partial T(l_c^+, t)}{\partial x}, \quad (3d)$$

$$\frac{\partial T(l_c + l_s, t)}{\partial x} = 0, \quad (3e)$$

$$\frac{\partial T(-l_b, t)}{\partial x} = 0, \quad (3f)$$

$$\lambda_b \frac{\partial T(0^-, t)}{\partial x} = f^-(0^-, t), \quad (3g)$$

$$\lambda_b \frac{\partial T(0^+, t)}{\partial x} = f^+(0^+, t), \quad (3h)$$

and

$$T(0^+, t) = T(0^-, t), \quad (3i)$$

where $f^+(0^+, t)$ is the portion of the total instantaneous heat flux flowing into the sample (side) and $f^-(0^-, t)$ is the portion of the total heat flux flowing into the base (side). Equations (3e) and (3f) are not generally applicable for the experimental system being modeled, but rather rely on conducting the experiments such that $T(l_c + l_s, t) = T(-l_b, t) = T_o$ for the duration of the experiment. It was assumed that this system of equations could not be solved analytically, and therefore a finite difference scheme based on the Crank-Nicholson method was constructed to replace it. Details of the scheme are provided in the Appendix.

Beyond the need for developing a numerical model of the heat transfer process, refinements were incorporated into the data reduction routine to account for the time constant of the thermocouple and the fact that the heat flux deviates from a true step function. Refining the temperature response model to account for the time constant of the thermocouple was necessitated by our use of Style I thermocouples to monitor the temperature at one juncture in this study. Though made from the same thickness of foil, Style I and Style II thermocouples have different geometries, and the time constant of Style I thermocouples ($t_c = 10 - 20$ ms) is longer than that of Style II thermocouples ($t_c = 2 - 5$ ms). This difference proved to be significant, the results derived from experiments with Style I and Style II thermocouples being different if the time constant was neglected. (This is in contrast to the case examined by MK, who found that the results obtained using 5- μ m- and 12- μ m-thick Style II thermocouples were the same and concluded that the time lag of the thermocouple response could be neglected.) To incorporate the effect of the time constant, we assumed that the response of the thermocouple to a unit step increase in temperature, $R(t)$, was associated with the form

$$R(t) = 1 - \exp(-t/t_c), \quad (4)$$

and we employed Duhamel's formula [15],

$$u(t) = \int_0^t R'(\tau) T(x, t - \tau) d\tau, \quad (5)$$

to express the response of the measurement system, $u(t)$ —i.e., the oscilloscope voltage reading—to the driving function $T(x, t)$ —i.e., the solution to equation(s) (3). This integral was incorporated into the system model by calculating $R'(\tau)T(x, t - \tau)$ at 0.001-ms intervals for $0 < \tau < t$ and using Simpson's rule to evaluate the integral. Corrected in this manner, the results obtained with Style I and Style II thermocouples were brought into agreement.

Regarding the refinement in the characterization of the heat flux, MK's analysis was based on the assumption that the heat generated in the foil was a true step function. That is, they

computed the ($I_o^2 r_f$, V_o^2 / r_f or $I_o V_o$) heat generated by the foil using two time-independent numbers: the foil's resistance, r_f , the nominal current, I_o , and/or the nominal voltage, V_o . Beyond being necessitated by the use of equation (1) for modeling the system, this approach is justified because small errors in the estimation of the heat flux make almost no difference in the thermal diffusivity values derived from the experiment. Moreover, the thermal conductivity and thermal diffusivity are effectively independent parameters, making the ratio of the thermal conductivity to the "measured" flux nearly a constant. Thus, the error in the thermal conductivity value scales directly with the error in the flux measurement. Since the $I^2 r_f$ or V^2 / r_f calculation of the heat generation is accurate to within 4% during the first 20 ms, and to within <1% for the remainder of the data acquisition period (see Figure 4), this approach to the flux calculation is warranted.

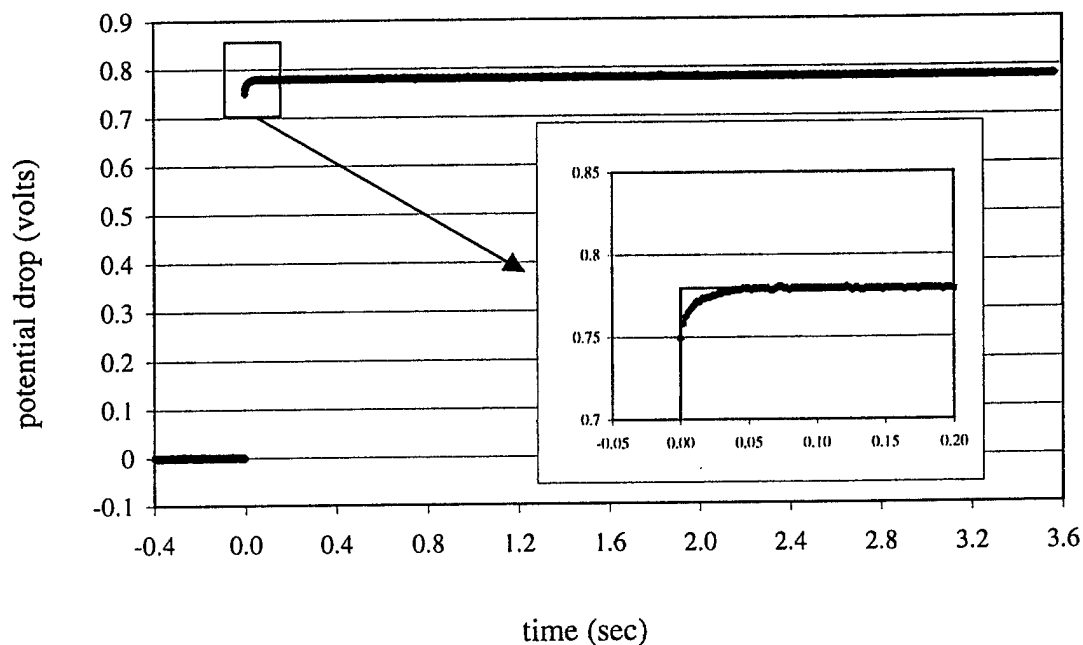


Figure 4. Voltage vs. Time Plot Associated With the Heat Generation Pulse.

Unfortunately, this attribute did not carry over to the configuration used in this study. In the course of analyzing the data for the results presented here, it was observed that small changes in assumed flux led to very large variations in the transport properties derived from the data. For

example, test-to-test variations in I_o/V_o —a measure of the uncertainty in the flux calculation—were observed to be on the order of 2%, and uncertainties of this magnitude translated into uncertainties of 20% or more in the value of the thermal conductivity. For this reason, it was considered necessary to employ a detailed characterization of the electrical energy delivered to the foil as a function of time. The use of a numerical model to simulate the process allowed this to be done. The computation of the heat flux was based on the instantaneous and nominal voltage drop “across the foil,” the nominal current, and the resistance of the foil using

$$f_o(t) = (I_o/V_o)^2 * V^2(t) * r_f / A, \quad (6)$$

where A is the area of the foil. While this improves matters, uncertainty in the computation of the heat flux remains a major issue in the viability of the technique. This issue is discussed further in section 5.

In order to facilitate fitting model simulations to the experimental data, the model was coupled to a nonlinear least-squares fitting routine. In performing the fit, all model parameters except T_o and λ_s were fixed at either measured or literature values, and the program was allowed to vary T_o and λ_s to minimize the root mean square of the residual. The fitting routine also identified the strong coupling of λ_s and α_s for all but the case where the specimen and base were the same material. This coupling necessitates that the specimen's ρ and c_p be known in order to derive λ_s and α_s . For this study, rather than measure ρ and c_p ourselves, we relied on literature values.

4. Results

Figure 5 shows experimental data from a representative test with a water sample, and a fit of the model of the heat transfer process to the test data. We note that a fast Fourier transform of the residual indicates that the noise is randomly distributed. Figure 6 shows a plot of measured thermal conductivity values vs. recommended literature values for water, ethylene glycol, and

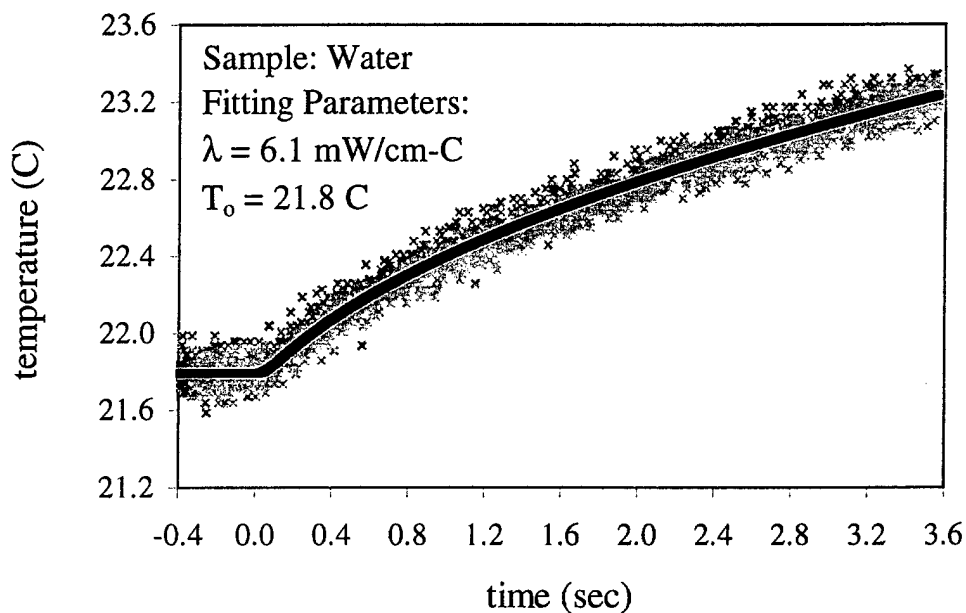


Figure 5. Temperature Response Observed in an Experiment With Water and the Fit of the Numerical Model to These Data.

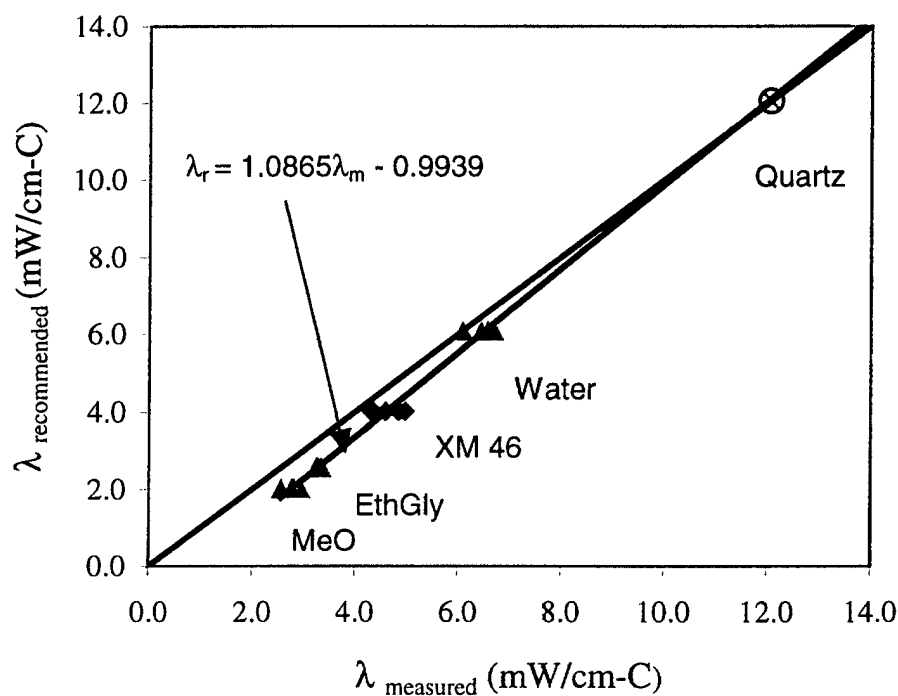


Figure 6. Plot of Measured Thermal Conductivity Values vs. Recommended Literature Values for Water, Ethylene Glycol, and Methanol (see Table 1).

methanol. It is observed that the measured values tend to be higher than those in the literature and that the discrepancy is larger for smaller values of thermal conductivity.

For the technique to be useful for characterizing unknowns, the source of the bias must either be incorporated into the model or the results adjusted empirically. In considering this matter, three potential sources of bias were identified. Of these, perhaps the most important is that the model neglects the heat up of the constantan foil. If the energy used to heat up the foil had instead been transferred into the base, the temperature rise would have been greater, and this would have resulted in the fitting routine deriving a lower thermal conductivity value. Another possible source of the bias may be the fact that the thermocouple couple leads are an unwanted heat sink. A sink would tend to lower the observed temperature increase, and this would indicate to the fitting routine that the sample had a higher conductivity than it actually has. A third possible source of the observed bias is convective cooling. Such an effect is not accounted for in the heat transfer model and, if non-negligible, would lead to an overprediction of thermal conductivity. Moreover, all of these effects would be larger for materials with lower thermal conductivity values because larger temperature increases and gradients are produced in the apparatus with these materials. (This is discussed more fully in section 5.)

In further considering this issue, it was noted that a linear least-squares fit of the data plotted in Figure 6 appears to well-represent the data and intersects with the diagonal near $12 \text{ mW/cm}^\circ\text{C}$ —the measured value of the fused silica sample and the point at which the least error would be expected. Thus, rather than try to incorporate the sources of bias into the model of the heat transfer process, we decided to use the results obtained for the standards as a basis for adjusting the results obtained for XM46. Based on five measurements near 23.5°C , the thermal conductivity for XM46 was measured to be $4.6 \text{ mW/cm}^\circ\text{C}$. Corrected for the systematic bias observed with the standards, a value $4.0 \text{ mW/cm}^\circ\text{C}$ is obtained. We have not conducted a rigorous error analysis because of the difficulty in estimating the uncertainties associated with various model input parameters. This value is in reasonable agreement with the value found by Messina et al. [9] ($3.5 \pm 0.6 \text{ mW/cm}^\circ\text{C}$ at 25°C) using a steady-state hot-wire technique [11]. A value of $3.5 \text{ mW/cm}^\circ\text{C}$ is also predicted from the theory of Bridgeman [16]:

$$\lambda = 3k v_s \left(\frac{\tilde{N}}{\tilde{V}} \right)^{2/3}, \quad (6)$$

where \tilde{N} is Avogadro's number, \tilde{V} is the molar volume, k is Boltzmann's constant, and v_s is the sonic velocity for the material. The sonic velocity for XM46 at 25° C and 0.1 MPa has been reported by Constantino [17] to be 1,940 m/s.

Figure 7 shows the thermal conductivity values we obtained for XM46 for temperatures in the range 20–60° C. Also shown are the measurements reported by Messina et al. [9] for this range, the values at 35, 40, and 50° C being acquired via a guarded hot plate technique. Their values vary little over this temperature range. Our values tend to fall below the values reported by Messina et al. [9] and indicate that XM46's thermal conductivity decreases with increase in temperature between 20 and 60° C. However, we observed the same trend with water, but its thermal conductivity is known to increase slightly over this temperature range (see Figure 7). While it is tempting to adjust our XM46 results based on this comparison, we do not believe that doing so is justified based on the work performed to date. Rather, we prefer to leave the question open at this time.

5. Discussion

The technique developed here may appear to be only a slight modification to the original MK concept, but the ramifications of the modifications are significant. To provide a clearer picture of the actual physical system being modeled and to show, at least qualitatively, the sensitivity of the temperature response to various input parameters, some case studies are provided. Figure 8 shows the calculated temperature response of a model system in which the "sample" has the same thermal transport properties as the base, in this case fused silica. The figure compares the results obtained using equation (1) and the numerical model described in the Appendix.

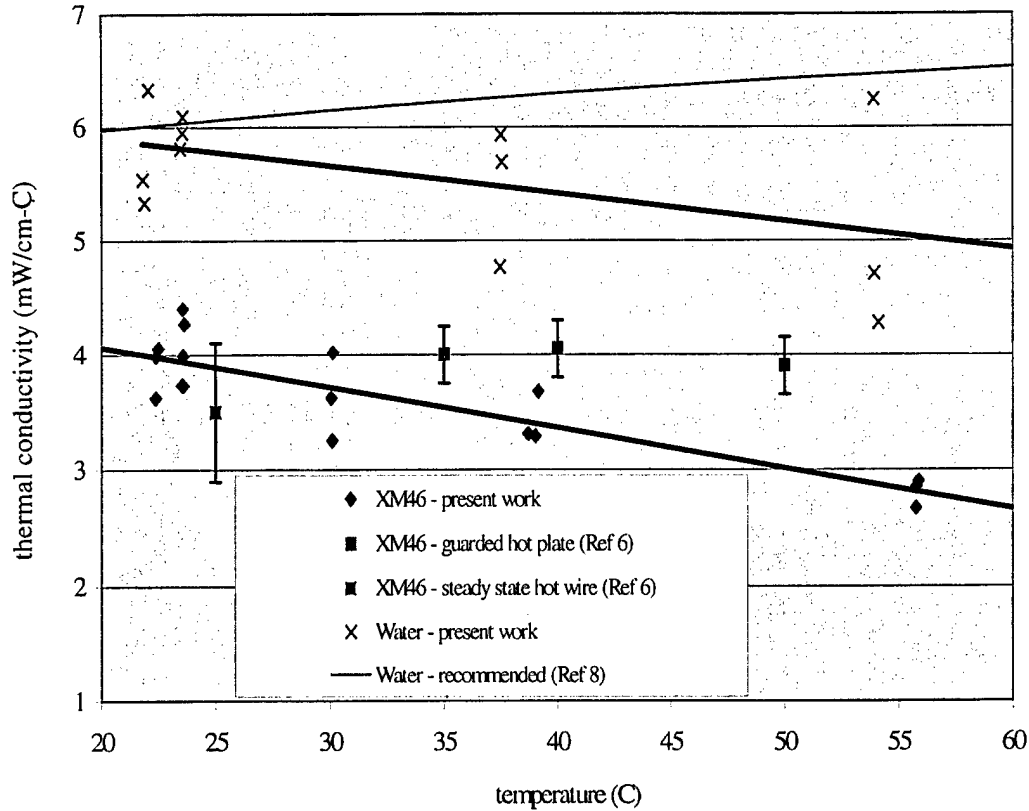


Figure 7. Measured Thermal Conductivity Values for XM46 and Water in the Range of 20–60° C.

These models are observed to be in good agreement. The results show that (as expected) the profiles on either side of the foil are identical. After 3.5 s, the temperature at the center is 1.85° C while the temperature at the thermocouple is 1.45° C. It is also worth noting that the temperature at the ends of the simulated sample (± 0.6 cm) are very near ambient, indicating the *de facto* appropriateness of model boundary conditions (3e) and (3f).

Figure 9 shows model temperature profiles generated with the same set of input parameters, but with a sample that has the thermal transport properties as methanol. Here the profiles are not symmetric about the foil, and the temperature increases at the foil and thermocouple are higher after 3.5 s than they are when fused silica is the sample. This is because methanol is a less effective heat sink than fused silica. As suggested by consideration of equation (2b), we have observed that a measure of the relative effectiveness of a material as a heat sink is $(\lambda \rho c_p)^{1/2}$.

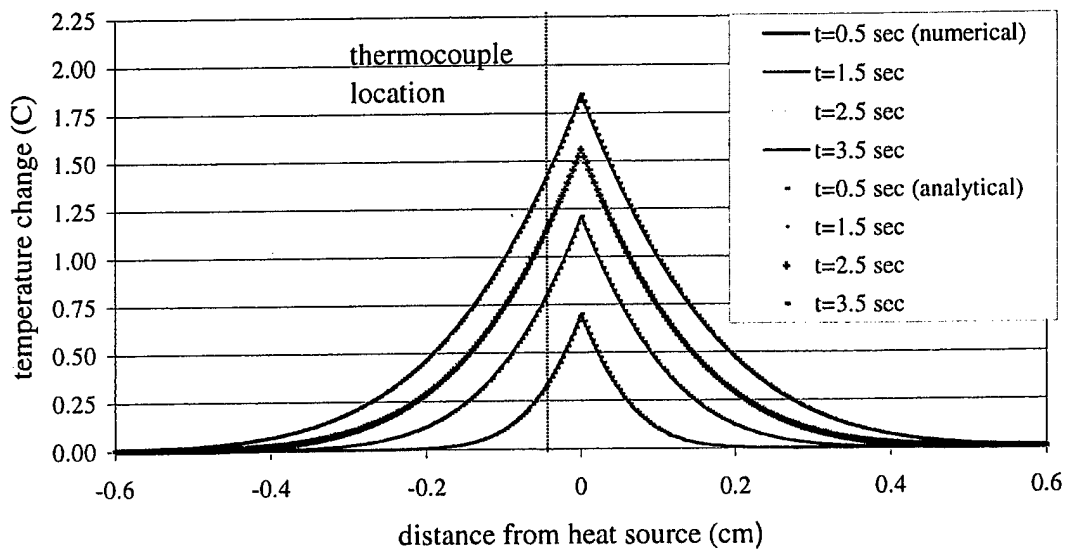


Figure 8. Spatial Temperature Profiles as a Function of Time for a Model System With a Fused Silica Sample ($f_o = 0.25 \text{ W/cm}^2$).

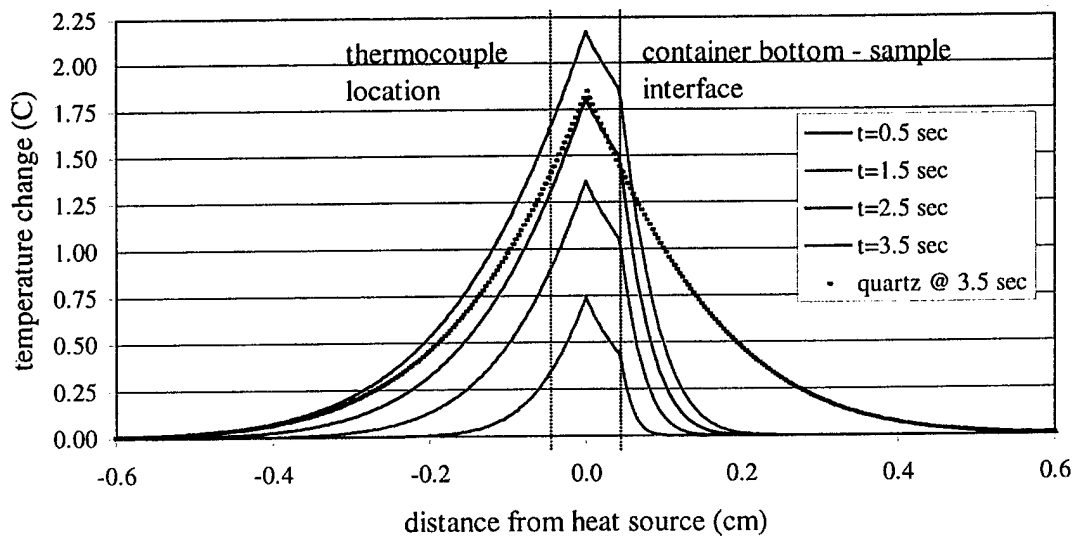


Figure 9. Spatial Temperature Profiles as a Function of Time for a Model System With a Methanol Sample ($f_o = 0.25 \text{ W/cm}^2$).

For example, the thermal conductivity of water (6 mW/cm-°C) is approximately half that of fused silica (12 mW/cm-°C). Thus, one might expect it to be a poor heat sink, and the temperature to respond in a manner similar to that observed for methanol. However, the value of $(\lambda\rho c_p)^{1/2}$ for water (0.16 J/°C-cm²-s^{1/2}) is slightly higher than that for fused silica (0.14 J/°C-cm²-s^{1/2}), and, as shown in Figure 10, the “measured” temperature increase is lower for the system with water than for the system with fused silica.

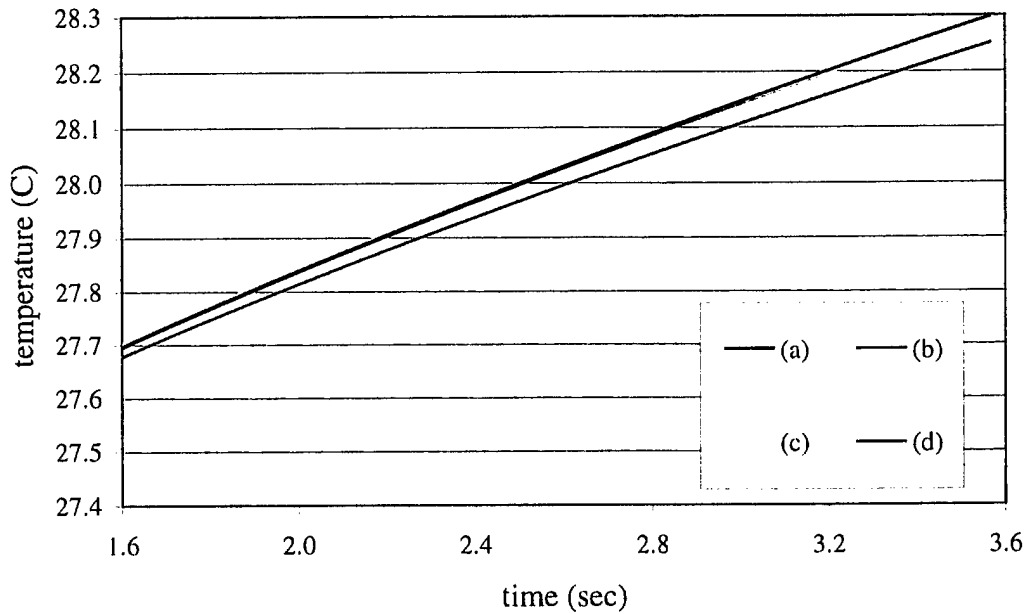


Figure 10. Temperature vs. Time Responses at the Thermocouple for Various Model Systems: (a) “Fused Silica,” $\lambda = 12.0 \text{ mW/cm-}^\circ\text{C}$, $r_f = 0.33 \ \Omega$; (b) “Water,” $\lambda = 6.1 \text{ mW/cm-}^\circ\text{C}$, $r_f = 0.33 \ \Omega$; (c) “Water,” $\lambda = 6.1 \text{ mW/cm-}^\circ\text{C}$, $r_f = 0.34 \ \Omega$; and (d) Fit to Simulation (c) Assuming $r_f = 0.33 \ \Omega$, the Fitting Routine Finding $\lambda = 4.8 \text{ mW/cm-}^\circ\text{C}$.

Figure 10 also compares the model responses for the case where (1) the material has the properties of water but the flux is based on a foil resistance of 0.34 Ω , and (2) these data are fit assuming the foil’s resistance is 0.33 Ω . The value of the thermal conductivity derived from the fit is 4.8 mW/cm-°C. This result highlights what we have found to be the main source of uncertainty in the experimental approach as developed to date—that is, the nonlinear relationship

between the temperature response and the heat flux. In this case, a 3% error in the flux calculation translates into a 21% error in the value of the conductivity derived from the experiment.

Part of the difficulty in characterizing the heat flux stems from the fact, recognized by Miller, that the voltage drop measured "across the foil" is associated with the sum of the resistance of the foil and a "contact resistance." To compute heat generation using $I^2 r_f$ or V^2/r_f , the contact resistance needs to be accounted for. However, it is not possible to independently quantify the contact resistance, the foil's resistance, and the instrument error on a test-to-test basis. Given that the contact resistance seemed the most likely parameter to vary significantly over the course of a test series, we decided to compute the instantaneous heat flux assuming that the resistance of the foil remained constant ($r_f = 0.33 \Omega$). Variations in the foil's resistance and instrument errors are not considered in the analysis. It was considered that a more detailed treatment of these errors would not significantly change the nominal values of transport properties derived from the experiment, but this should be verified in future work.

The first and most obvious improvement that can be made to the experiment is to modify the numerical simulation of the heat transfer process to include the heat up of the foil. This could be done using the PC-based compiler (Microsoft FORTRAN) employed for this study by utilizing data files rather than dimensioned arrays for some of the variables employed in the computation. (This approach was used to permit instantaneous voltage readings to be employed in the calculation of the heat flux.) Nonuniform grid spacings might also prove beneficial. Another option is to employ a compiler that facilitates the specification of larger dimensioned arrays. But each of these options entails effort that is beyond current mission interests, and they are left for future work.

The possibility of reducing the impact of small variations in model input parameters should also be investigated. The experiment developed to this point is a result of decisions based on availability of materials, our ability (and limitations) in constructing pieces from the available

material, and our experience in selecting variables such as the temporal duration of the transient, the magnitude of the heat flux, and the thickness of various pieces. The magnitude of the heat flux, the duration of the record, and the thickness of the pieces are constrained by several factors. As currently configured, the random noise in the thermocouple reading is about $\pm 0.2^\circ \text{C}$. With this amount of noise, temperature increases of at least several degrees are desirable. Larger temperature increases can be achieved by (1) increasing the magnitude of the heat flux, (2) recording the transient for longer times, and (3) making the thermocouple-foil distance as small as possible. But large temperature increases are undesirable because the property of interest may be temperature-dependent. Also, if the heat flux is too large or the transient too long, the ability to achieve consistency between the boundary conditions of the model and actual systems will be difficult to maintain. To better address this issue, the parameter space of the heat transfer process needs to be explored to identify if there are conditions under which the experiment can be run such that small variations in input parameters do not lead to large variations in the derived result.

6. Summary

A technique has been developed to measure the thermal conductivity of small electrically conductive liquid or solid samples. The viability (and limitations) of the technique, which is a modification of the one developed by MK for the study of small energetic solid materials, was established through experiments with water, methanol, and ethylene glycol. The technique was employed to establish thermal conductivity values for XM46 in the range $20\text{--}60^\circ \text{C}$ ($4 \text{ mW/cm}^\circ\text{C}$ at 23.5°C). It was hoped that the technique would provide a reasonable in-house capability for acquiring such information. However, at its current stage of development, results are a very sensitive function of the input parameters needed to fit the data, and considerable work is required to achieve reliable values. Some improvements should be realizable, but it is not certain that further dedicated development of the technique is warranted.

7. References

1. Miller, M. S., and A. J. Kotlar. "Technique for Measuring the Thermal Diffusivity/Conductivity of Small Thermal Insulator Specimens." *Review of Scientific Instruments*, vol. 64, pp. 2954–2960, 1993.
2. Miller, M. S., and A. J. Kotlar. "A New Technique for the Simultaneous Measurement of Thermal Diffusivity and Thermal Conductivity of Small Energetic-Material Specimens." ARL-TR-1321, U.S. Army Research Laboratory, Aberdeen Proving Ground, MD, 1997.
3. Carlslaw, H. S., and J. C. Jaeger. *Conduction of Heat in Solids*. London: Oxford University Press, 1959.
4. McQuaid, M. J., A. Kinkennon, R. A. Pesce-Rodriguez, and R. A. Beyer. "Laser-Based Ignition for a Gunfire Simulator (GUFS): Thermal Transport Properties for Candidate Igniter Materials." Technical report, U.S. Army Research Laboratory, Aberdeen Proving Ground, MD, to be published.
5. Miller, M. S. "Thermal Conductivities and Diffusivities of Solid Gun Propellants." *Combustion, Science and Technology*, vol. 100, pp. 345–354, 1994.
6. Miller, M. S. "Thermophysical Properties of Six Solid Gun Propellants." ARL-TR-1322, U.S. Army Research Laboratory, Aberdeen Proving Ground, MD, 1997.
7. Miller, M. S. "Thermophysical Properties of Cyclotrimethylenetrinitramine." *Journal of Thermophysics and Heat Transfer*, vol. 8, pp. 803–805, 1994.
8. Miller, M. S. "Thermophysical Properties of RDX." ARL-TR-1322, U.S. Army Research Laboratory, Aberdeen Proving Ground, MD, 1997.
9. Messina, N. A., M. Tarczynski, C. A. Spiegel, and L. S. Ingram. "Characterization of Hydroxylammonium Nitrate (HAN) Based Liquid Monopropellants, Part 2. – Physical and Thermal Properties Measurements." PCRL-FR-92-005, Princeton Combustion Research Laboratory, Fort Monmouth, NJ, 1992.
10. Miller, M. S. "Step Function Current in a Metallic Foil as a Step Function Heat Flux Source." *Journal of Applied Physics*, vol. 72, pp. 3904–3907, 1992.
11. Ramires, M. L. V., C. A. Hieto de Castro, Y. Nagasaka, A. Nagashima, M. J. Assael, and W. A. Wakeham. "Standard Reference Data for the Thermal Conductivity of Water." *Journal of Chemical Reference Data*, vol. 24, pp. 1377–1381, 1995.

12. Touloukian, Y. S., P. E. Liley, and S. C. Saxena (eds.). "Thermophysical Properties of Matter." *Thermal Conductivity: Non-Metallic Liquids and Gases*, vol. 3, New York: IFI/Plenum, 1970.
13. Perry, R. H., and C. H. Chilton (eds.). *Chemical Engineer's Handbook*. Fifth edition, New York: McGraw-Hill, 1973.
14. Messina, N. "The Role of Physical Properties in Dynamic Loading Processes and Bubble Collapse of Liquid Monopropellants for LGP Application." *21st JANNAF Combustion Subcommittee Meeting*, CPIA Publication 412, 1984.
15. Wylie, C. R. *Advanced Engineering Mathematics*. Fourth edition, New York: McGraw-Hill, 1975.
16. Bridgeman, P. W. *Proceedings of the American Academy of Arts and Science*. Vol. 59, pp. 141-169, 1923.
17. Constantino, M. "The High Pressure Equation of State of LPG1845 and LPG1846." *Proceedings of the 1986 JANNAF Propulsion Meeting*, CPIA Publication 455, vol. 1, 1986.

Appendix:

Numerical Simulation of the Heat Transfer Process

INTENTIONALLY LEFT BLANK.

Having assumed that the differential equations describing the dynamics of the heat transfer process could not be solved analytically, the equations were replaced with a set of finite difference equations based on the Crank-Nicholson implicit method.¹ Referring to Figure A-1, the general replacement equations are

$$-r^{(\pm)}T(i-1, j+1) + (2/\alpha^{(\pm)} + 2r^{(\pm)})T(i, j+1) - r^{(\pm)}T(i+1, j+1) = \\ r^{(\pm)}T(i-1, j) + (2/\alpha^{(\pm)} - 2r^{(\pm)})T(i, j) + r^{(\pm)}T(i+1, j),$$

where i and j are spatial and temporal indices, respectively, and the superscripts refer to whether x is greater than (+) or less than (-) zero, these regimes being calculated independently. The parameter r is a function of the temporal (Δt) and spatial (Δx) increments,

$$r^{(\pm)} = \Delta t / [\Delta x^{(\pm)}]^2.$$

The temporal increment is fixed, somewhat arbitrarily, to be half the value of the time between experimental data points. For the work presented in this report, a data point was acquired every 0.002 s, so the simulation time step was 0.001 s. This increment is small relative to the time scale of the dynamics of the heat transfer process and is convenient from the standpoint of using Simpson's rule to numerically integrate equation (5). The spatial increment is left (at least initially) to the discretion of the user. Due to compiler-limited array sizes, a maximum of 350 (spatial) grid points are available to resolve the temperature profile. (The user can choose to use less.) Of the number of points selected, half are assigned to the base side ($x < 0$) and half to the sample side ($x > 0$). For the sample side, the spatial increment (Δx^+) is calculated by dividing the actual thickness of the container bottom by a user-specified number ($i_m - 1/2$). For the base side, the spatial increment (Δx^-) is calculated by dividing the thickness of wafer separating the foil and the thermocouple by this same number. The length of the (simulated) sample is therefore

¹ Smith, G. D. *Numerical Solution of Partial Differential Equations: Finite Difference Methods*. 3rd edition, New York: Oxford University Press, 1985.

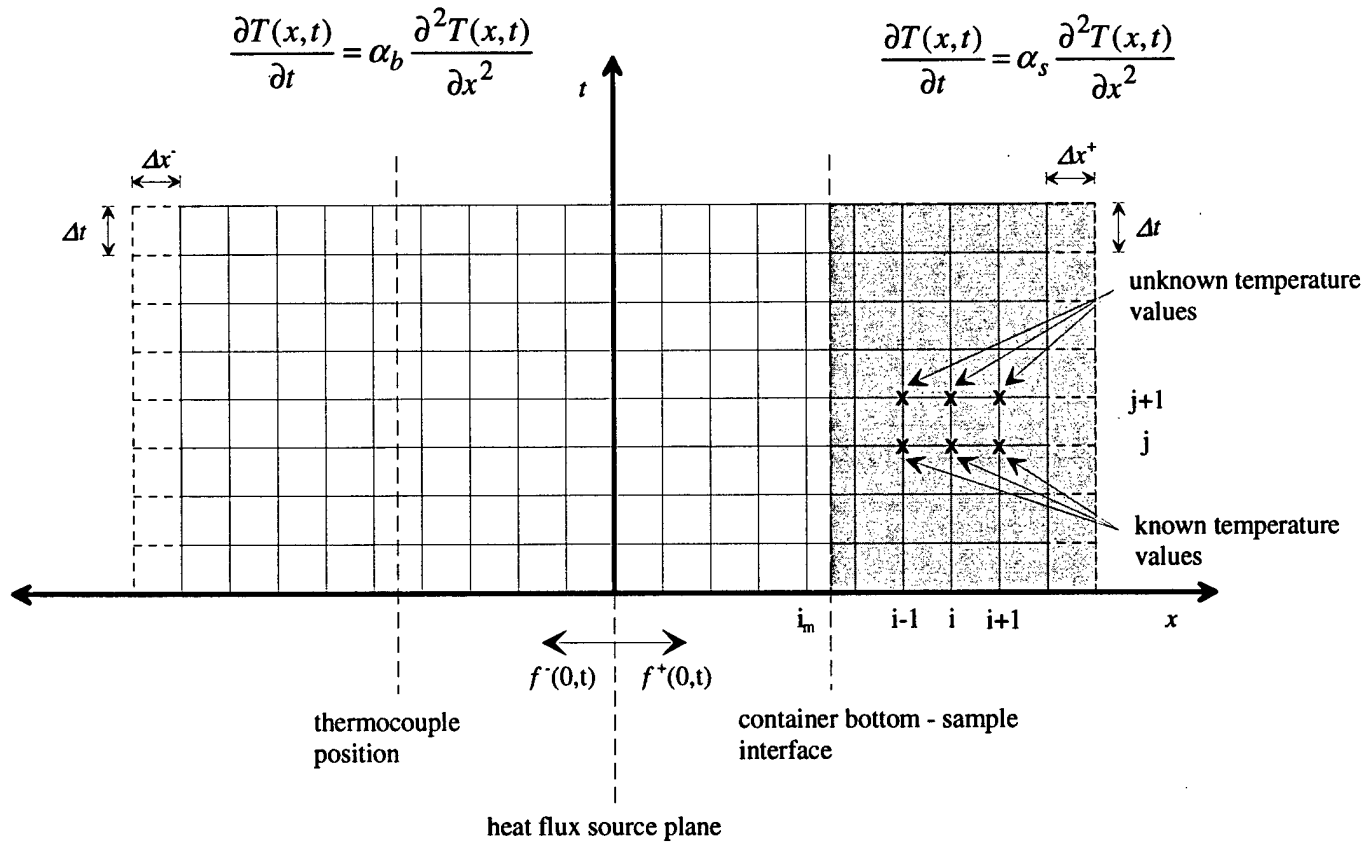


Figure A-1. Pictorial Representation of Numerical Model Parameters.

$(i_{max}-i_m)\Delta x^+$, where i_{max} is the number of points assigned to a side. The length of the base is $(i_{max}-1/2)\Delta x^-$. The selection of i_m involves a compromise between achieving reasonable spatial resolution for the temperature profile in the container bottom and ensuring that the (simulated) sample length is long enough so that boundary condition $\frac{\partial T(l_c+l_s)}{\partial x}=0$ is met—i.e., $T(l_c+l_s) \sim T_o$ —but not so long that it exceeds the length of the sample employed in the experiment.

The replacement equations associated with boundary conditions (3e) and (3f) are

$$-r^+T(i_{max}-1, j+1) + \left(\frac{2}{\alpha_s} + r^+\right)T(i_{max}, j+1) = -2r^+T(i_{max}-1, j) + \left(\frac{2}{\alpha_s} - 2r^+\right)T(i_{max}, j)$$

and

$$-rT(i_{max}-1, j+1) + \left(\frac{2}{\alpha_b} + r\right)T(i_{max}, j+1) = -2rT(i_{max}-1, j) + \left(\frac{2}{\alpha_b} - 2r\right)T(i_{max}, j),$$

respectively. However, since these boundary conditions are not a general feature of the experimental system, but rather rely on the conditions under which the tests are run, it is incumbent on the user to adjust the value of i_m such that the conditions $T(i_{max}, j_{max}) \approx T_o$ and $i_{max}\Delta x^+ < l_s$ are met. Toward this end, the nonlinear least-squares fitting routine was written to return $T(i_{max}, j_{max})$ and l_s as output. In addition, the program will override the user's selection of i_m if the stability criterion for the Gaussian elimination procedure used to solve the system of equations is not met. To ensure physical realism, the criterion $(2/\alpha - 2r > 0)$ is checked and i_m changed automatically if necessary. The values $i_m = 13$ and $i_{max} = 175$ were used to obtain all the results reported here.

At the interface between the container bottom and the sample, conservation of energy requires that the temperatures on either side of the boundary be related to the temperature at the boundary, $T(i_m + 1/2, j)$, per

$$T(i_m + 1/2, j) = \frac{\lambda_b T(i_m, j) + \lambda_s T(i_m + 1, j)}{\lambda_b + \lambda_s}.$$

This relationship leads to the replacement equations

$$\begin{aligned} -rT(i_m - 1, j+1) + \left(\frac{2}{\alpha_b} + \frac{r(\lambda_b + 3\lambda_s)}{\lambda_b + \lambda_s}\right)T(i_m, j+1) - \left(\frac{2r\lambda_s}{\lambda_b + \lambda_s}\right)T(i_m + 1, j+1) = \\ -rT(i_m - 1, j) + \left(\frac{2}{\alpha_b} - \frac{r(\lambda_b + 3\lambda_s)}{\lambda_b + \lambda_s}\right)T(i_m, j) - \left(\frac{2r\lambda_s}{\lambda_b + \lambda_s}\right)T(i_m + 1, j) \end{aligned}$$

and

$$\begin{aligned} -\left(\frac{2r\lambda_b}{\lambda_b + \lambda_s}\right)T(i_m, j+1) + \left(\frac{2}{\alpha_s} + \frac{r(3\lambda_b + \lambda_s)}{\lambda_b + \lambda_s}\right)T(i_m + 1, j+1) - rT(i_m + 2, j+1) = \\ -\left(\frac{2r\lambda_b}{\lambda_b + \lambda_s}\right)T(i_m, j) + \left(\frac{2}{\alpha_s} - \frac{r(3\lambda_b + \lambda_s)}{\lambda_b + \lambda_s}\right)T(i_m + 1, j) - rT(i_m + 2, j). \end{aligned}$$

Boundary conditions (3g) and (3h) present a challenge because the partitioning of the flux, $f_o(0,t)$, into f^- and f^+ is not known *a priori* and the partitioning changes with time. (More energy will flow to the side with the more effective heat sink, and the difference will increase with time.) To resolve this issue, an iterative approach was developed to determine the partitioning of energy that would satisfy the boundary condition $T(0^+,t) = T(0^-,t)$. This entails making an initial guess at the partitioning, independently computing the temperature profiles for $x < 0$ and $x > 0$, comparing $T(0^+,t)$ and $T(0^-,t)$, and selecting a new partitioning if the condition $T(0^+,t) - T(0^-,t) \leq 1 \times 10^{-7} \text{ }^\circ\text{C}$ is not met. A secant root finding method was developed to abet the search process. The subroutine written to implement this method is a slightly modified version of the program found in Press et al.² During a cursory monitoring of the efficacy of the search process, it was observed that the convergence criteria were always met within two passes, and that $T(0^+,t) - T(0^-,t)$ was less than $1 \times 10^{-12} \text{ }^\circ\text{C}$.

² Press, W. H., B. P. Flannery, S. A. Teukolsky, and W. T. Vetterling. *Numerical Recipes: The Art of Scientific Computing (FORTRAN Version)*, Cambridge: Cambridge University Press, 1989.

List of Abbreviations

Nomenclature

α	thermal diffusivity (square centimeters/second)
Δt	temporal increment (seconds)
Δx	spatial increment (centimeters)
λ	thermal conductivity (watts/centimeter•degrees Celsius)
ρ	density (grams/cubic centimeter)
u_s	sonic velocity (centimeters/second)
A	area of the foil (square centimeters)
c_p	heat capacity (joules/gram•degrees Celsius)
f_o	heat flux (watts/square centimeter)
I_o	nominal current of electrical pulse employed to heat foil (amperes)
i	spatial index
j	temporal index
k	Boltzmann's constant
l	length (centimeters)
\tilde{N}	Avogadro's number
r	$\Delta t/(\Delta x)^2$ (seconds/square centimeter)
r_f	resistance of foil (ohms)
$R(t)$	temporal response of passive system to a unit step forcing function
T_o	ambient temperature (degrees Celsius)
$T(x,t)$	actual temperature (degrees Celsius)
$u(t)$	measured temperature (degrees Celsius)
\tilde{V}	molar volume (cubic centimeters/gram)
V_o	nominal drop in electric potential (volts)
$V(t)$	instantaneous drop in electric potential (volts)
x	distance from heat source (centimeters)

Subscripts

b	base material property
s	specimen property
m	index for spatial grid point
max	total number of spatial grid points associated with one side of the foil

Superscripts

+	values for $x > 0$
-	values for $x < 0$

INTENTIONALLY LEFT BLANK.

<u>NO. OF COPIES</u>	<u>ORGANIZATION</u>
2	DEFENSE TECHNICAL INFORMATION CENTER DTIC DDA 8725 JOHN J KINGMAN RD STE 0944 FT BELVOIR VA 22060-6218
1	HQDA DAMO FDQ D SCHMIDT 400 ARMY PENTAGON WASHINGTON DC 20310-0460
1	OSD OUSD(A&T)/ODDDR&E(R) R J TREW THE PENTAGON WASHINGTON DC 20301-7100
1	DPTY CG FOR RDE HQ US ARMY MATERIEL CMD AMCRD MG CALDWELL 5001 EISENHOWER AVE ALEXANDRIA VA 22333-0001
1	INST FOR ADVNCD TCHNLGY THE UNIV OF TEXAS AT AUSTIN PO BOX 202797 AUSTIN TX 78720-2797
1	DARPA B KASPAR 3701 N FAIRFAX DR ARLINGTON VA 22203-1714
1	NAVAL SURFACE WARFARE CTR CODE B07 J PENNELLA 17320 DAHLGREN RD BLDG 1470 RM 1101 DAHLGREN VA 22448-5100
1	US MILITARY ACADEMY MATH SCI CTR OF EXCELLENCE DEPT OF MATHEMATICAL SCI MAJ M D PHILLIPS THAYER HALL WEST POINT NY 10996-1786

<u>NO. OF COPIES</u>	<u>ORGANIZATION</u>
1	DIRECTOR US ARMY RESEARCH LAB AMSRL DD J J ROCCHIO 2800 POWDER MILL RD ADELPHI MD 20783-1145
1	DIRECTOR US ARMY RESEARCH LAB AMSRL CS AS (RECORDS MGMT) 2800 POWDER MILL RD ADELPHI MD 20783-1145
3	DIRECTOR US ARMY RESEARCH LAB AMSRL CI LL 2800 POWDER MILL RD ADELPHI MD 20783-1145
	<u>ABERDEEN PROVING GROUND</u>
4	DIR USARL AMSRL CI LP (305)

NO. OF
COPIES ORGANIZATION

ABERDEEN PROVING GROUND

29 DIR USARL
AMSRL WM B
A W HORST
AMSRL WM BD
B E FORCH
W R ANDERSON
R A BEYER
S W BUNTE
C F CHABALOWSKI
S COLEMAN
A COHEN
R DANIEL
D DEVYNCK
R A FIFER
B E HOMAN
A JUHASZ
A J KOTLAR
K L MCNESBY
M MCQUAID (2 CPS)
M S MILLER
A W MIZIOLEK
J B MORRIS
J E NEWBERRY
R A PESCE-RODRIGUEZ
P REEVES
B M RICE
R C SAUSA
M A SCHROEDER
J A VANDERHOFF
AMSRL WM BE
A BIRK
C LEVERITT

REPORT DOCUMENTATION PAGE			Form Approved OMB No. 0704-0188	
<small>Public reporting burden for this collection of information is estimated to average 1 hour per response, including the time for reviewing instructions, searching existing data sources, gathering and maintaining the data needed, and completing and reviewing the collection of information. Send comments regarding this burden estimate or any other aspect of this collection of information, including suggestions for reducing this burden, to Washington Headquarters Services, Directorate for Information Operations and Reports, 1215 Jefferson Davis Highway, Suite 1204, Arlington, VA 22202-4302, and to the Office of Management and Budget, Paperwork Reduction Project(0704-0188), Washington, DC 20503.</small>				
1. AGENCY USE ONLY (Leave blank)		2. REPORT DATE March 1999		3. REPORT TYPE AND DATES COVERED Final, May - Oct 98
4. TITLE AND SUBTITLE A Technique for Determining Thermal Transport Properties of Small, Electrically Conductive Liquid or Solid Specimens			5. FUNDING NUMBERS 1L161102AH43	
6. AUTHOR(S) Michael McQuaid and Max Cohen*				
7. PERFORMING ORGANIZATION NAME(S) AND ADDRESS(ES) U.S. Army Research Laboratory ATTN: AMSRL-WM-BD Aberdeen Proving Ground, MD 21005-5066			8. PERFORMING ORGANIZATION REPORT NUMBER ARL-TR-1905	
9. SPONSORING/MONITORING AGENCY NAMES(S) AND ADDRESS(ES)			10. SPONSORING/MONITORING AGENCY REPORT NUMBER	
11. SUPPLEMENTARY NOTES *Mr. Cohen worked as a 1998 Summer Intern at the U.S. Army Research Laboratory.				
12a. DISTRIBUTION/AVAILABILITY STATEMENT Approved for public release; distribution is unlimited.			12b. DISTRIBUTION CODE	
13. ABSTRACT (Maximum 200 words) The experimental approach developed by Miller and Kotlar for determining the thermal conductivity and thermal diffusivity of small, solid, energetic-material specimens—"Technique for Measuring the Thermal Diffusivity/Conductivity of Small Thermal Insulator Specimens," <i>Review of Scientific Instruments</i> , vol. 64, pp. 2954-2960, 1993—has been modified and extended for use in determining these properties for electrically conductive materials, including liquids. As in the technique developed by Miller and Kotlar, these properties are determined from the transient temperature response of a point in an experimental system consisting of two "semi-infinite" media, a plane of which is subjected to a well-defined heat flux. However, to allow the technique to be employed with electrically conductive specimens, the experiment is configured so that the heat flux is generated at a plane in a nonconductive solid (as opposed to the interface between the media), and the temperature response is measured in this solid as well. The parameter $(\lambda\rho c_p)^{1/2}$ is obtained by fitting a numerical simulation of the heat transfer process to the temperature response. Coupling the model to a nonlinear least-squares fitting routine facilitates this effort. To obtain absolute values for the specimen's thermal conductivity and thermal diffusivity, knowledge of its density and heat capacity is required. The viability of the experimental approach was established through experiments with water, methanol, and ethylene glycol, and the technique was employed to obtain the thermal conductivity of liquid propellant XM46 for temperatures in the range 20–60° C.				
14. SUBJECT TERMS XM46, thermal conductivity			15. NUMBER OF PAGES 37	
			16. PRICE CODE	
17. SECURITY CLASSIFICATION OF REPORT UNCLASSIFIED	18. SECURITY CLASSIFICATION OF THIS PAGE UNCLASSIFIED	19. SECURITY CLASSIFICATION OF ABSTRACT UNCLASSIFIED	20. LIMITATION OF ABSTRACT UL	

INTENTIONALLY LEFT BLANK.

USER EVALUATION SHEET/CHANGE OF ADDRESS

This Laboratory undertakes a continuing effort to improve the quality of the reports it publishes. Your comments/answers to the items/questions below will aid us in our efforts.

1. ARL Report Number/Author ARL-TR-1905 (McQuaid) Date of Report June 1999

2. Date Report Received _____

3. Does this report satisfy a need? (Comment on purpose, related project, or other area of interest for which the report will be used.) _____

4. Specifically, how is the report being used? (Information source, design data, procedure, source of ideas, etc.) _____

5. Has the information in this report led to any quantitative savings as far as man-hours or dollars saved, operating costs avoided, or efficiencies achieved, etc? If so, please elaborate. _____

6. General Comments. What do you think should be changed to improve future reports? (Indicate changes to organization, technical content, format, etc.) _____

CURRENT
ADDRESS

Organization

Name

E-mail Name

Street or P.O. Box No.

City, State, Zip Code

7. If indicating a Change of Address or Address Correction, please provide the Current or Correct address above and the Old or Incorrect address below.

OLD
ADDRESS

Organization

Name

Street or P.O. Box No.

City, State, Zip Code

(Remove this sheet, fold as indicated, tape closed, and mail.)
(DO NOT STAPLE)